CARBOWASTE

Treatment and Disposal of Irradiated Graphite and Other Carbonaceous Waste

Grant Agreement Number: FP7-211333

- Report (WP 6 Task 6.1.7) –

Report on the carbon suboxide and hydrogenated carbonaceous deposits: synthesis, characterization and dissolution properties

N. Toulhoat, A. Blondel, N. Moncoffre, N. Bérerd

Institut de Physique Nucléaire de Lyon – CNRS/IN2P3 – Université Lyon 1

Date of issue of this report: April 2013

Start date of the project : **01/04/2008** Duration : **60 Months**

Project co-funded by the European Commission under the Seventh Framework Programme (2007 to 2011) of the European Atomic Energy Community (EURATOM) for nuclear research and training activities

Dissemination Level

PU	Public	
RE	Restricted to the partners of the CARBOWASTE project	**x**
CO	Confidential, only for specific distribution list defined on this document	

Distribution list

Person and organisation name and/or group	Comments
CARBOWASTE Project Participants	

CARBOWASTE		
Work package: 6 **Task: :** 6.1.7	**CARBOWASTE document no:**	**Document type: D**
Issued by: IPNL **Internal no.:**		**Document status:** Final

Document title

Report on the carbon suboxide and hydrogenated carbonaceous deposits: synthesis, characterization and dissolution properties

Executive summary

Graphite components which have been irradiated in a CO_2-based coolant are likely to display the occurrence of carbon deposits. These deposits may result from the polymerisation of C_3O_2 derived from the radiolysis of carbon monoxide. They may also result from the radiolytic destruction of methane, if this component is present in the coolant gas (principally in AGRs plus some French reactors). The main drawbacks related to an excess of the formation of the carbon deposits are the reduction of the heat exchange performances and an important increase in neutron capture. Moreover, the presence of the deposits needs also to be taken into account because they are susceptible to retain radioactive species such as ^{14}C and even ^{36}Cl. The understanding of the formation, the chemical form, the location and the behavior of the carbon deposits is important to take into account during decommissioning where dusts might be generated. In case of dismantling under water or to determine the future disposal options it is also important to check their resistance to leaching.

After an introduction and a short overview on the nature, the formation and properties of carbon deposits formed in UNGG, AGR or MAGNOX type reactors, we focus on the synthesis, through gas irradiation, of two types of deposits, carbon suboxide and hydrogenated carbonaceous deposits. The characterization of these deposits is presented, using several techniques and finally, their dissolution properties are addressed. The main conclusions that can be drawn from this work are that carbon suboxide deposits are highly soluble in pure water but their occurrence in reactors should be rather scarce because of their thermal lability. Concerning the hydrogenated carbonaceous deposits, they are much more stable but almost not soluble in pure water.

Revisions						
Rev.	Date	Short description	Author	Internal Review	Task Leader	WP Leader

Table of contents

1 Introduction :

Many studies have been carried out on the carbon deposits in the frame of the UNGG or MAGNOX and AGR nuclear reactors. These deposits are of different kinds and they may be formed on metallic parts or on graphite [J.Wright 1980]. The carbon deposits located on the metallic parts may have complex structures: filamentous, amorphous or graphite platelets [R.T.K.Baker 1972]. The relative rates of formation of each type depend on temperature. In UNGG reactors the temperature of the metallic parts (200 to 700°C) favors the formation of filamentous carbon deposits.

Two kinds of deposits may occur: Carbon suboxides deposits (mainly occurring on the cold parts of the moderator) and hydrogenated carbonaceous deposits (mainly occurring on the warm parts of the moderator) [LeJeune et al. 1974, T.Baird et al. 1980, P.Campion 1980]. The two probable sources of the carbon deposit are methane and carbon monoxide, which are added to the carbon dioxide gas coolant to reduce the radiolytic oxidation of the graphite moderator. Carbon suboxides result from the radiolytic polymerisation of C_3O_2 whereas hydrogenated carbon deposits are mainly produced through the radiolytic destruction of CH_4. The presence of the first one has been noted in MAGNOX reactors while the presence of the second one has been noted in the reactors where CH_4 was added to the cooling gas (principally AGRs plus some French reactors such as Bugey for instance) [EPRI Technical Report 2006].

The formation of the deposits is catalyzed by transition metals such as iron, nickel, cobalt and chromium as well as by aluminum. But it is inhibited by silica, silicon carbide, copper, gold and steel [J.Wright 1980 ; T.Baird et al. 1980 ; R.L.Faircloth et al. 1980].

The main drawbacks related to the formation of the carbon deposits are the reduction of the heat exchange performances and an important increase in neutron capture. As a matter of fact, an excess of these components on fuel cladding and heat exchanger surfaces may result in lowering heat transfer efficiency and raising fuel pin temperatures [G.C. Allen et al. 1997]. Moreover, the irradiation of CH_4 leads to the formation of H_2 and finally to the incorporation

of hydrogen into the hydrogenated carbon deposits (around 1%) favoring therefore the increase in neutron capture [R.Blanchard et al. 1969 ; R.Blanchard et al. 1971].

The thermal reactivity of these deposits in air is up to 1000 times greater than that of graphite. Their quantities are generally small, however their distribution around the core is quite variable and locally, in MAGNOX type reactors, the amounts can reach up to 3% by weight of the associated graphite in the worst case. Blanchard et al [R.Blanchard et al. 1969] have shown that at a temperature of 380°C and a pressure of 52 bars, a concentration of 730 vpm of CH_4 irradiated with gammas of 7.5 W g^{-1} in the Belgian reactor BR 2 leads within one hour to a production of 8 à 12 ppm of hydrogenated carbon deposits.

Consequently, the presence of the deposits needs to be taken into consideration in decommissioning where, for example, flame cutting of adjacent metallic structures is contemplated, and also where dusts may be generated [EPRI Technical Report 2006].

Moreover, the presence of the deposits needs also to be taken into account because they are susceptible to retain radioactive species such as ^{14}C (through incorporation or ion exchange, [Faucitano et al. 1977]) and even ^{36}Cl. Indeed, an experience of Yvars et al. [M.Yvars et al. 1973] has shown that the gamma irradiation of a graphite sleeve put in CO_2 at a pressure of 40 bars (deposited energy around 2-3 W.g^{-1}) leads to the formation of a carboxide deposit that "trapped" around 71 ppm chlorine.

Thus, the understanding of the formation, the chemical form, the location and the behavior of the carbon deposits is essential to determine the future disposal options. In this latter context as well in the frame of underwater dismantling, it is also important to check their resistance to leaching.

2 Literature data on the formation and resistance to oxidation and radiolytic corrosion of carbon deposits:

2.1 Carbon suboxides deposits:

The carbon suboxides are formed through the radiolysis of CO that results in the formation of C_3O_2 and CO_2. At reactor temperatures, C_3O_2 polymerizes and forms rust colored deposits on graphite with pulverulent carbon particles [M.Schmidt 1964 ; A.Dyer and G.E.Moores 1977 ; J.Wright 1980 ; C.J.Wood 1980 ; P.Campion 1980 ; A.Blanchard and P.Campion 1980 ; R.L.Faircloth et al. 1980 ; D.J.Norfolk et al. 1980a ; D.J.Norfolk et al. 1980b ; D.J.Norfolk et al. 1983]. Their structure is amorphous like, close to the structure of carbon black obtained through hydrocarbon cracking. These deposits are porous with a high specific surface (100 to 200 $m^2.g^{-1}$). Their thermal conductivity is low [M.Yvars et al. 1973].

Carbon suboxide has been synthetized as astrophysical ice analogs consisting primarily of carbon suboxide ice (C_3O_2) as well as, in the context of gas cooled nuclear reactors, analogs of carbon suboxide deposits. It is one of the most stable polycarbon oxides of the series C_nO_2 [C.J. Bennett et al. 2008]. It was generally produced from the irradiation of its precursor, carbon monoxide, using UV electron, gamma or ion irradiation [T. Baird 1972, C.J. Bennett et al. 2008].

The irradiation of carbon monoxide leads to the formation of $(C_3O_2)_n$ polymer through following reactions :

$$CO + CO \rightarrow CO_2 + C,$$
$$C + 2\ CO \rightarrow C_3O_2\ (gas),$$
$$n(C_3O_2)\ (gas) \rightarrow (C_3O_2)_n$$

Balanced reaction: $4\ CO \rightarrow CO_2 + C_3O_2$

The C_3O_2 compound polymerizes on solid substrates as a rusty colored deposit with following structure defined by Smith at al. [R.N. Smith et al. 1963]:

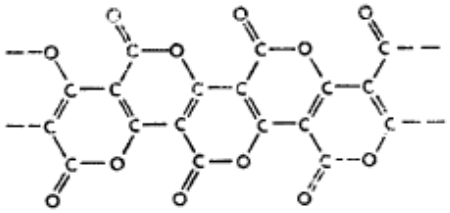

A.R. Blake et al. [A.R. Blake et al. 1963] have made an IR spectroscopic analysis of a carboxide deposit obtained through dehydration of malonic acid and obtained following spectrum:

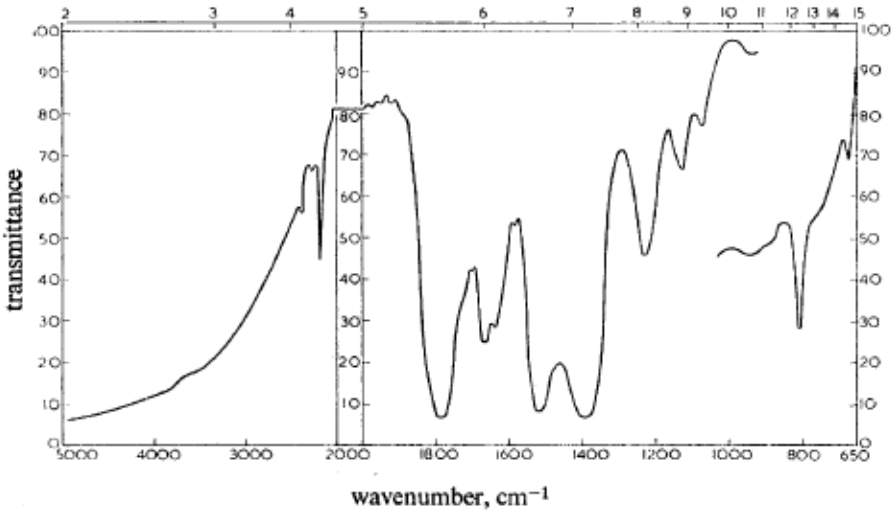

The resistance of carboxide deposits to thermal oxidation has been tested by Yvars et al. [M. Yvars et al 1973] in CO_2 with 230 vpm of O_2 at a pressure of 1 bar. At a temperature of 300°C the consumption is around 50% and reaches 80% at 500°C. As the oxidation follows an Arrhenius law, the consumption should be completed at a temperature around 600°C. Therefore, the injection of oxygen allowed burning the carboxide deposits in certain French reactors (such as CHA2) whereas it allowed burning only partially the hydrogenated deposits [Lejeune et al. 1974; Lejeune et al.1975].

2.2 Hydrogenated carbonaceous deposits:

The hydrogenated carbonaceous deposits formed through the radiolysis of CH_4 on the warm parts of the moderator bricks, are black colored and honeycombed structured. The radiolysis of CH_4 results in a major incidence on the mechanical and neutronic characteristics of the nuclear graphite [M.Yvars et al. 1973; A.J.Wickham et al. 1977; A.Dyer and Moores 1977 ; C.J.Wood 1980]. The radiolytic methane destruction is influenced by temperature and the Arrhenius plots show the existence of two regimes, a low and a high temperature regime [A.Dyer and.E.Moores 1977]. At reactor temperatures lower than 400°C, the activation energy corresponding to the first regime is lower than 4 $kJ.mol^{-1}$ whereas above 600°C, the activation energy of the second regime is of 81 $kJ.mol^{-1}$.

The irradiation of the cooling gas leads to the oxidation of methane and the resulting species are mainly ethane and propane through following reactions [J.Brisbois and C.Fiche 1967 ; P.Campion 1980].

$$CH_4 + CO_2 \xrightarrow{h\upsilon} CH_2$$
$$CH_2 + CH_4 \rightarrow C_2H_6$$
$$CH_2 + C_2H_6 \rightarrow C_3H_8$$

The oxidation of the alkanes finally leads to the formation of the hydrogenated carbonaceous deposits on graphite. The precursors of these deposits are unsaturated hydrocarbons such as residues of ethylene (C_2H_3) or acetylene (C_2H_2) [C.W.Keep et al. 1980; D.J.Norfolk et al. 1980a ; D.J.Norfolk et al. 1980b]. CO and H_2O hinder the formation of the deposits because they can react with the activated CO_2 to form cation clusters. The kinetics of the formation of these deposits increases with the temperature and increases linearly with the concentration of methane. It is also proportional to the square root of the energy deposited by gamma radiation [R.Blanchard et al. 1969].

The radiolytic corrosion of hydrogenated deposits becomes significant at temperatures around 600°C even if the total consumption is never reached. It is proportional to their porosity and is similar to that observed on graphite [R.Blanchard et al. 1971]. The consumption grows first

linearly with their quantity and finally flattens. It is also more difficult to achieve if the deposits have been formed at high temperatures [R.Blanchard et al. 1969].

3 Experimental:

We have synthesized analogs of both types of deposits using ion irradiation of carbon monoxide on one hand and a mixture of methane and carbon dioxide (50/50) on the other hand. The irradiations have been performed using the external beamline of the 4 MV Van de Graaff accelerator of IPNL. Two dedicated irradiation cells have been used: 1) a cell allowing the deposition of carbon suboxide at room temperature on the internal walls of the cell or on a glass slide and nuclear graphite sample introduced into the cell; 2) a cell allowing the deposition of a hydrogenated carbonaceous deposit on a heated nickel foil. The heating of the nickel foil has been used to catalyze the formation of the deposit.

3.1 Carbon suboxides deposits:

3.1.1 Synthesis:

A 304L stainless steel irradiation cell was used to synthesize the deposits. This cell was placed on the external beam line of the 4MV Van de Graaff accelerator facility of IPNL. The irradiation device and the cell have been described by Pichon et al. [C. Pichon 2006]. The beam is extracted from the vacuum of the beamline into the irradiation cell through a 10 µm thick Havar foil. A cross section of the cell is presented in Figure 1. The cell is equipped with three tappings allowing its pre-emptying, gas loading and continuous pressure measurement. The cell was filled with CO (4.7-Q) gas at a pressure around 2 bars. The energy of the incident particles was around 7.5 MeV and after extraction through the Havar foil, it was around 4.4 MeV. The irradiation lasted around 10 hours and the dose deposited into the gas was of 25 MGy.

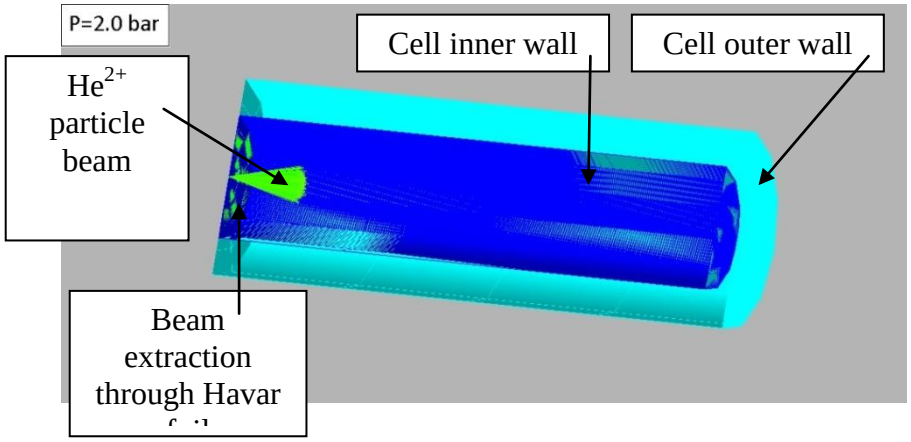

Figure 1: Cross section of the irradiation cell used for the irradiation of CO gas

The irradiation led to the formation of a rusty colored deposit on the inner walls of the cell presented on the optical image in Figure 2.

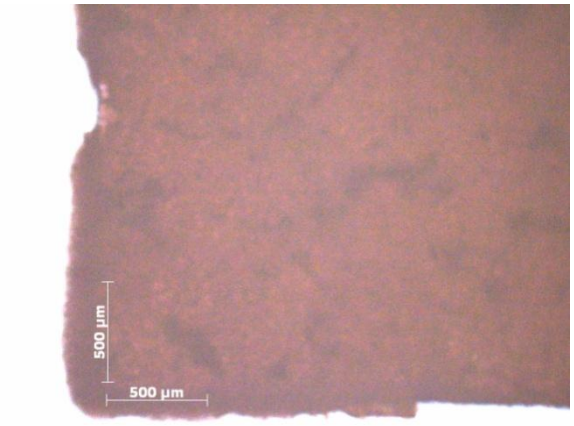

Figure 2: Optical image of the deposit formed by CO irradiation with He^{2+} particles

3.1.2 Characterization:

3.1.2.1 FT IR spectroscopy

The deposit was first analyzed by FT IR at the "Ecole Supérieure de Chimie Physique Electronique de Lyon (CPE)". The sample was analyzed on KBr discs using a Nicolet Impact 410 FTIR Spectrometer. The corresponding spectrum is presented in Figure 3.

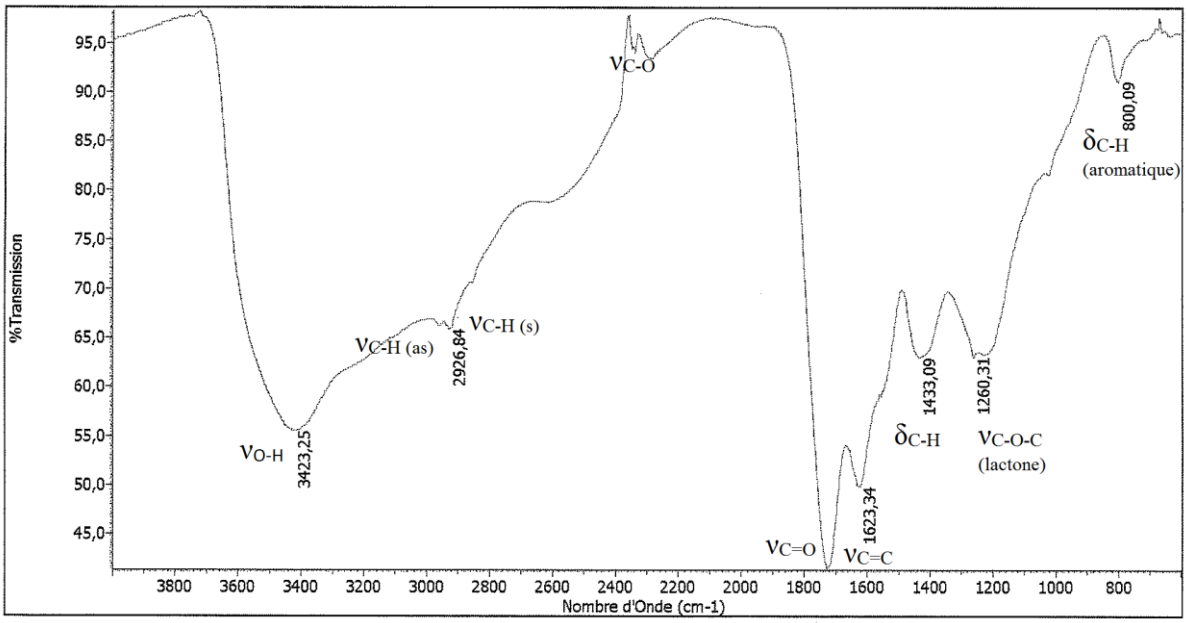

Figure 3: IR spectrum of the deposit synthesized by CO irradiation with He^{2+} particles

The most intense absorption peak located at 1750 cm^{-1} corresponds to the vibration of the C = O group present in lactones. This is confirmed by the peak at 1260 cm^{-1} corresponding to the vibration of the C – O – C group. Moreover, the band at 1623 cm^{-1} is identified as the vibration of the C = C groups in a cyclic structure. The absorption peaks at 2338 cm^{-1} are attributed to the symmetric and asymmetric vibrations of the C-O groups of CO_2. The large band beyond 2500 cm^{-1} and the absorption peaks at 1402 cm^{-1} and 800 cm^{-1} correspond to vibrations of C – H and O – H groups.

After heating of the deposit at 150°C during 8 hours, the following spectrum was obtained (Figure 4).

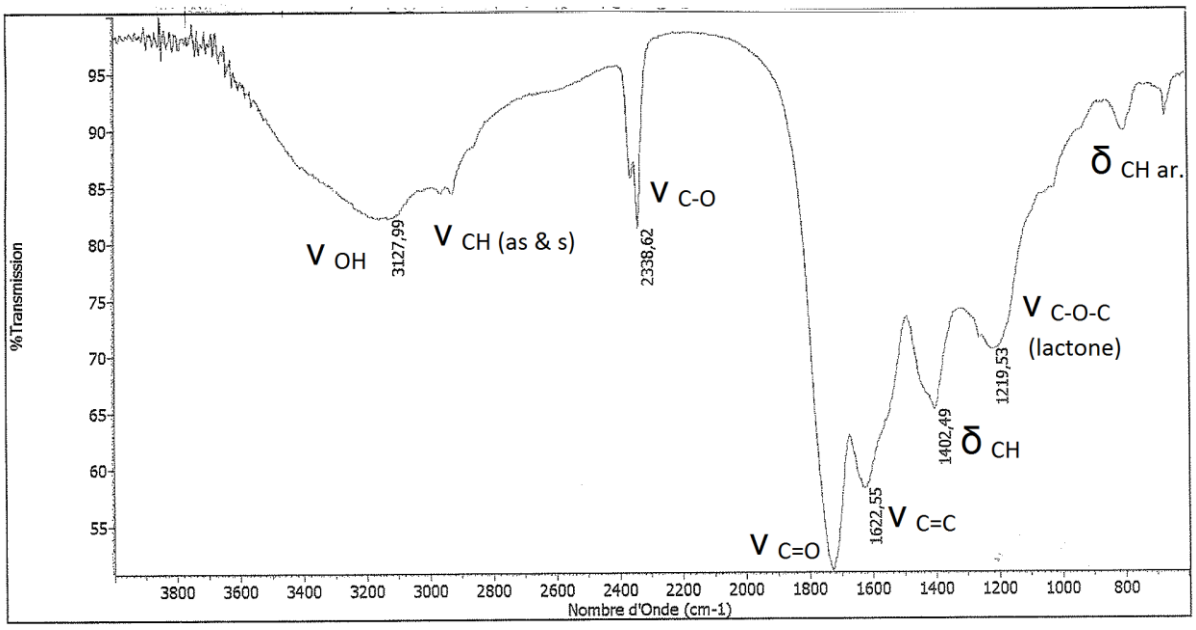

Figure 4: IR spectrum of the deposit synthesized by CO irradiation with He^{2+} particles heated at 150°C during 8 hours

The drop of the absorption band located between 3800 and 2400 cm^{-1} is related to the loss of water adsorbed on the suboxide (due to its hygroscopic character) and evaporated during heating. Moreover, the growing of the absorption peak located at 2338 cm^{-1} shows that the structure of the deposit breaks down with temperature. The formation of CO_2 might correspond to the opening of the aromatic rings.

The experiments allow concluding that the structure of the synthesized deposit seems to be close to that synthesized by A.R. Blake et al. [A.R. Blake et al. 1963] (section 1) corresponding to $(C_3O_2)_n$.

3.1.2.2 Rutherford Backscattering Spectrometry (RBS):

A second irradiation has been performed by irradiating a CO gas put in contact with a glass slide as well as with a nuclear graphite sample introduced into the irradiation cell. This allowed the deposition of thick rusty colored deposits on the slide and on the graphite with thicknesses reaching several micrometers. The deposit has been analyzed by RBS using a 2

MeV incident He^{2+} beam at the 4 MV Van de Graaff accelerator of IPNL. The particles were detected with a silicon surface barrier detector at a detection angle θ of 172°. Figure 5 represents the experimental spectrum together with spectrum fitted with SIMNRA [M. Mayer, SIMNRA] obtained on the graphite sample. This spectrum shows that the main constituents of the deposits are carbon (around 32 at.%) and oxygen (around 23 at.%) and that the deposit incorporated a certain amount of Fe, Cr, Co (less than 1at.%). It must be noted that the fitting of the spectrum needed to take into account around 45 at.% hydrogen. Figure 6 represents the carbon and oxygen depth profiles. This figure shows that the carbon and oxygen concentrations are homogeneous on a thickness around 400 nm. The carbon concentration increase correlated to the oxygen concentration decrease shows that the deposit penetrates into the graphite pores.

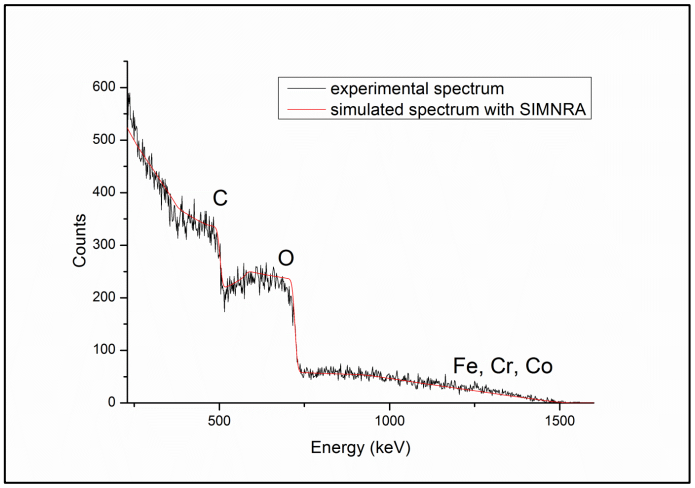

Figure 5: RBS (He^{2+}, 2 MeV) experimental and fitted spectra of the deposit

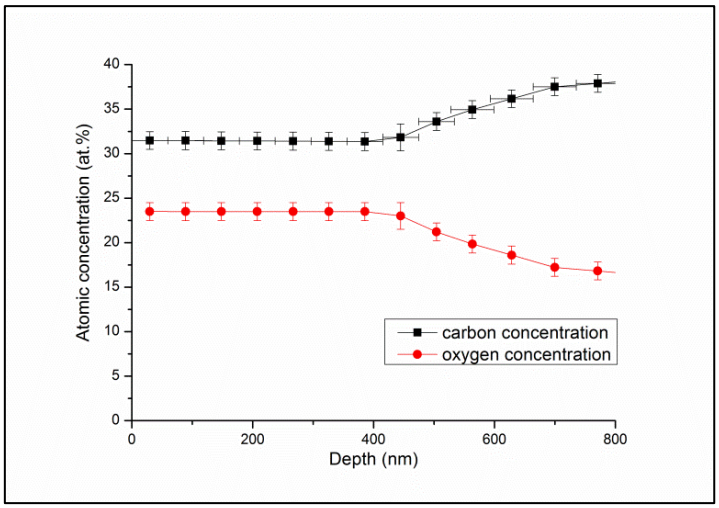

Figure 6: Carbon and oxygen depth profiles in the carbon suboxide deposit formed on the nuclear graphite sample assuming a density of 1.5 for the deposit.

3.1.2.3. Nuclear Magnetic Resonance spectroscopy (NMR)

In order to get more insight into the carbon and hydrogen speciation, the deposit has been analyzed by NMR at the "Centre de Résonance Magnétique Nucléaire à très hauts champs (CRMN)" of Lyon. The experiments were carried out by Dr. Anne Lesage. All NMR experiments were carried out on a Bruker AVANCE III spectrometer operating at a ^{1}H Larmor frequency of 800.13 MHz. The proton spectra were referenced to the single resonance observed in adamantane for protons at 1.87 ppm with respect to neat tetramethylsilane (TMS). ^{13}C chemical shifts were referenced with respect to the CH_2 resonance of adamantane at 38.48 ppm with respect to neat TMS [C.R. Morcombe et al. 2003]. All spectra were recorded at a spinning frequency of 22 kHz, using a 3.2 mm probe.

-Carbon-13 CPMAS spectra (800 MHz, 22 kHz MAS) showed that the recorded signal to noise ratio in CP. 1D spectra was too weak to get reliable information on carbon.

- Proton spectra (800 MHz, 22 kHz MAS) show that:

i) There are four main peaks at 6.8 ppm, 3.2 ppm, 1.3 mm and 0.34 ppm (Figure 7).

ii) Proton-double quantum (DQ) experiments clearly show that the main peak (peak A) correspond to isolated protons (-XH groups) as this resonance is filtered out from the DQ one-

dimensional spectrum. The chemical shift at 6.8 ppm is in agreement with aromatic like protons (=CH) or phenolic like protons (=C-OH) (Figure 8).

iii) The peak at 3.2 ppm (peak B) likely corresponds to water molecules, as it gives a strong auto-correlation peak in the DQ-SQ correlation spectrum at (3.2 ppm / 6.4 ppm) but is absent in the TQ-filtered 1D spectrum (Figure 9).

iv) Peaks C and D correspond to aliphatic hydrocarbons.

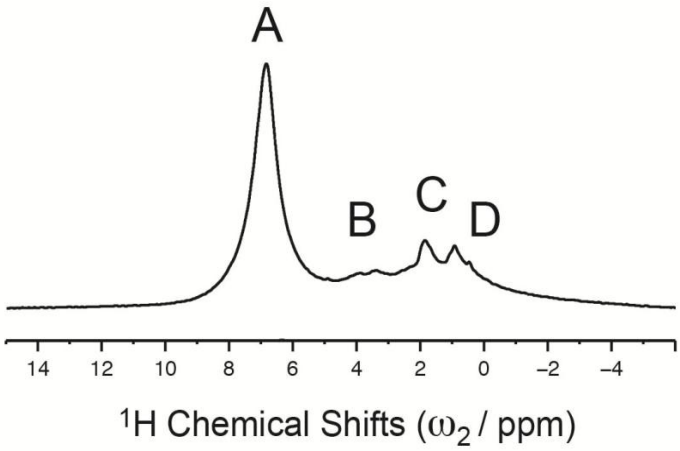

Figure 7: Simple Quantum spectrum of the deposit

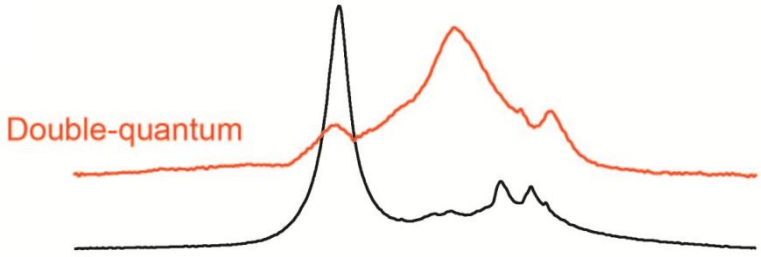

Figure 8: Double Quantum spectrum compared to the Simple Quantum one

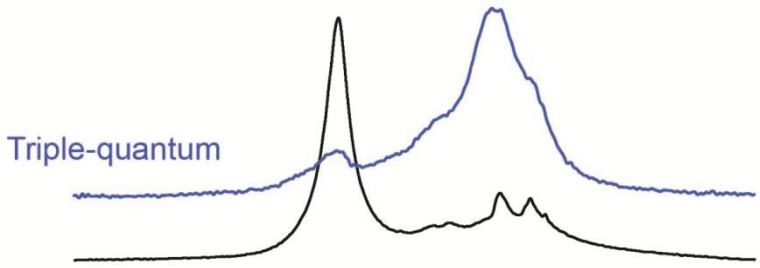

Figure 9: Triple Quantum spectrum compared to the Simple Quantum one

Finally, this experiment allowed showing that the hydrogen molecules do not take part in the structure but correspond mainly to isolated protons or aromatic or phenolic like protons as well as adsorbed water molecules.

3.2 Hydrogenated carbonaceous deposits:

3.2.1 Synthesis:

The synthesis of the hydrogenated carbonaceous deposits has been carried out on a different irradiation cell that was also placed on the external beamline of the 4 MV Van de Graaff accelerator facility of IPNL and the beam was extracted from the vacuum of the beamline into the cell through a 10µm thick Havar window. This cell is equipped with tappings allowing the pre-emptying of the cell, gas loading and continuous pressure measurement as well as on line gas analysis. The cell is made of brass and coated with a thin gold layer and can be equipped with two sample holders allowing two different irradiation configurations: i) a position where the sample is vertical allowing irradiating both gas + sample, i.e. the beam stops at the gas/sample interface; ii) a horizontal one where the sample is not irradiated and the beam stops into the gas. The sample holder is made of boron nitride with a thin embedded graphite wire allowing heating the sample holder up to 600°C. The temperature is controlled through a small thermocouple inserted between the sample and the sample holder. Both irradiation configurations are presented schematically in 10 and 11.

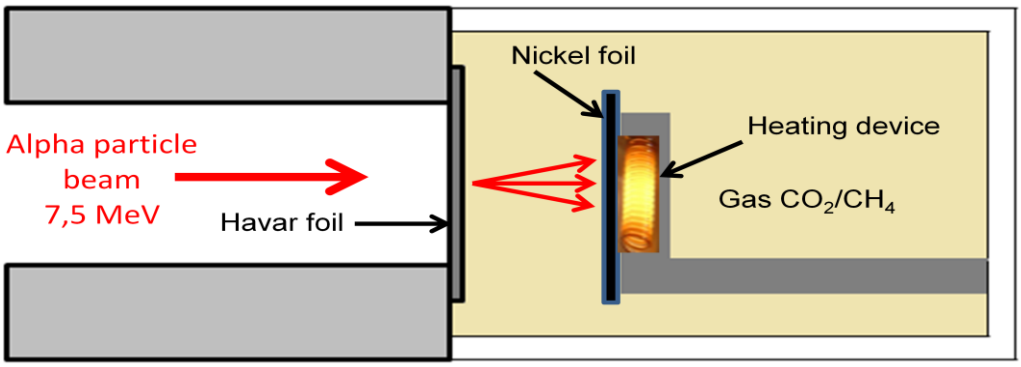

Figure 10: Scheme of the irradiation cell used for the synthesis of the hydrogenated carbonaceous deposits (sample + gas irradiation)

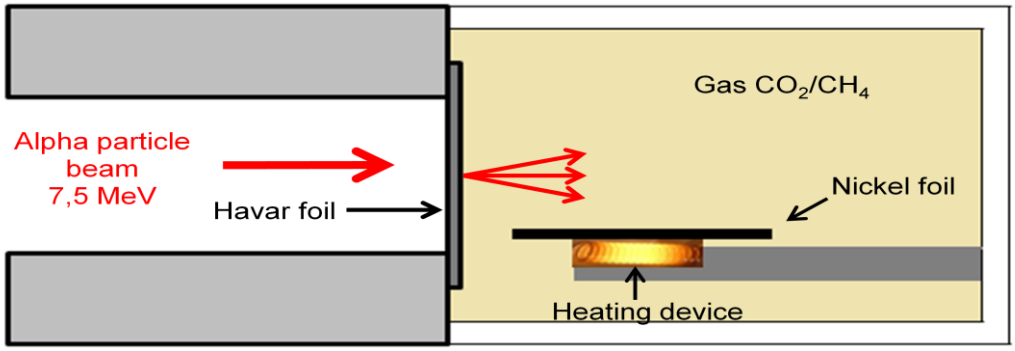

Figure 11: Scheme of the irradiation cell used for the synthesis of the hydrogenated carbonaceous deposits (gas irradiation without sample irradiation)

The cell was filled with a mixture of 50% CO_2 and 50% CH_4 in both cases and a nickel foil was placed on the sample holder and heated to 500°C. The irradiation experiments were carried out with a 7.5 MeV He^{2+} particle beam that entered the cell with an energy around 4.4 MeV after the Havar window. In both cases the gas was irradiated during around 6 hours and the dose deposited into the gas was around 30 MGy. The evolution of the gas composition was monitored by using a gas microcrochromatography analyser (µGC), mounted by SRA Instruments, coupled to a mass spectrometer (MS 5975C inert MSD Agilent Technology). The µGC is equipped with three capillary columns (MS5A, PLOTU and OV1), allowing the

separation of molecules from He to heavy C4-C8 hydrocarbons, and the gaseous molecules are detected with a Thermal Conductivity Detector (TCD).

Both irradiation configurations led to a black deposit on the nickel foil that catalyzed its formation. The deposit is not homogeneous when the foil is not irradiated (Figure 12) whereas it is uniformly spread on the nickel foil when the beam stopped at the gas/nickel interface (Figure 13). No deposition occured on the inner part of the cell walls.

Figure 12: black deposit on the nickel foil (foil not irradiated)

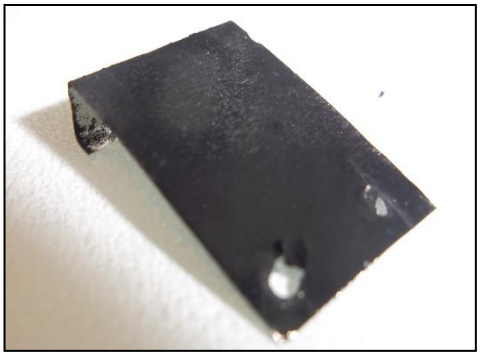

Figure 13: nickel foil uniformly covered with a black deposit (foil irradiated)

In order to ckeck the formation of the deposits on graphite, another experiment was carried out by irradiating a mixture of 50% CO_2 and 50% CH_4 together with a sample of Highly Ordered Pyrolitic Graphite (HOPG). The sample was put in a vertical position as mentioned above in i) allowing irradiating both gas + sample, i.e. the beam stopped at the gas/HOPG interface.

The gas was irradiated during around 6 hours and the dose deposited into the gas was around 30 MGy. This irradiation resulted in the formation of a non uniform distribution of carbonaceous deposits with generally less than 50 µm diameter “urchin-shaped” deposits generally preferentially located on fractures of (001) surfaces (Figure 14).

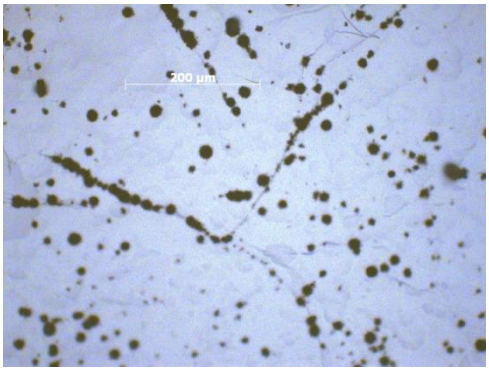

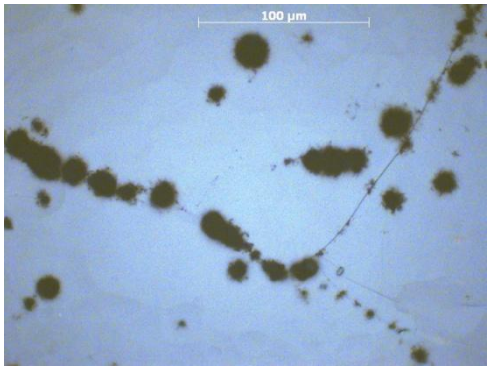

Figure 14 left and right: Optical microscope pictures of the carbonaceous deposits formed on HOPG surface after irradiation of both the gas mixture and the HOPG surface

3.2.2 Characterization:

3.2.2.1 Gas analysis

A first irradiation was performed without any nickel sample. During this irradiation, the evolution of the irradiated gas composition was monitored. The irradiation led to the consumption of CH_4 and CO_2 and to the production of H_2 and showed that with increasing irradiation dose, new and heavier hydrocarbon species were formed. These heavy molecules are the precursors leading to the formation of the observed carbonaceous deposit.

Table 1 resumes the molecules appearing for doses ranging from 0.5 to 8 MGy and Figure 15 represents the evolution of all gaseous species in the irradiated gas for doses up to 10 MGy.

	Name	Chemical formula	Observations
1	Ethane	C_2H_6	Formation from 0 to 0.5 MGy
2	Propane	C_3H_8	Formation from 0 to 0.5 MGy
3	Dimethyl ether	CH_3OCH_3	Formation from 0 to 0.5 MGy
4	Isobutane	C_4H_{10}	Formation from 1 MGy
5	Butane	C_4H_{10}	Formation from 0 to 0.5 MGy
6	Neopentane	C_5H_{12}	Formation from 2 MGy
7	Methoxyethane	C_3H_8O	Formation from 4 MGy
8	Ethanol	CH_3CH_2OH	Formation from 4 MGy
9	Acetone	CH_3COCH_3	Formation from 4 MGy
10	2-methylbutane	C_5H_{12}	Formation from 0.5 MGy
11	Isopropylalcohol	C_3H_8O	Formation from 6 MGy
12	2-methoxypropane	$C_4H_{10}O$	Formation from 4 MGy
13	Pentane	C_5H_{12}	Formation from 4 MGy
14	3-methoxy-2-butanol	$C_5H_{12}O_2$	Formation from 8 MGy
15	2-methylpropanal	C_4H_8O	Formation from 6 MGy
16	2,2-dimethylbutane	C_6H_{14}	Formation from 4 MGy
17	Propanol	C_3H_8O	Formation from 8 MGy

Table 1 : Resume of the gaseous compounds formed during the irradiation of a CH_4/CO_2 (50/50) mixture with 4.4 MeV He^{2+} particles

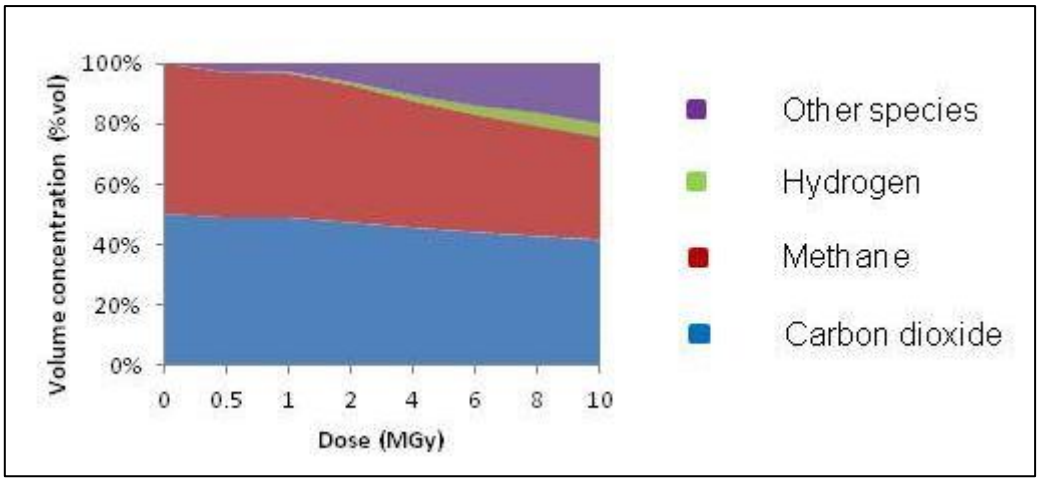

Figure 15: Evolution of all gaseous species in the irradiated gas mixture CH_4/CO_2 (50/50) for doses up to 10 MGy

3.2.2.2 Non Rutherford Elastic Scattering Spectrometry (NRBS) and Elastic Recoil Detection Analysis (ERDA)

The deposit uniformly spread on the nickel foil after irradiating gas+nickel foil was analysed by NRBS and ERDA at the 4 MV VDG accelator facility of IPNL. As conventional RBS was not suited for the detection of light elements in the thin carbonaceous film deposited on the nickel substrate, we used NRBS at an incident He^{2+} energy of 7.5 MeV and a detection angle θ of 172°. More specifically, this energy corresponds to a resonance energy of the $^{16}O(He^{2+}, He^{2+})^{16}O$ reaction and allows therefore enhancing the oxygen signal. ERDA was used to analyse hydrogen with an incident He^{+} beam of 1.7 MeV. In this case, the H recoil nucleus was used to determine the distribution profile of hydrogen. The incident beam angle was equal to 15° and the detection angle θ was 30°. A 6.5 µm thick mylar foil was placed in front of the detector in order to stop the backscattered He^{+} particles.

The experimental spectra and simulated spectra (using SIMNRA) obtained by NRBS and ERDA are respectively presented on Figures 16 and 17.

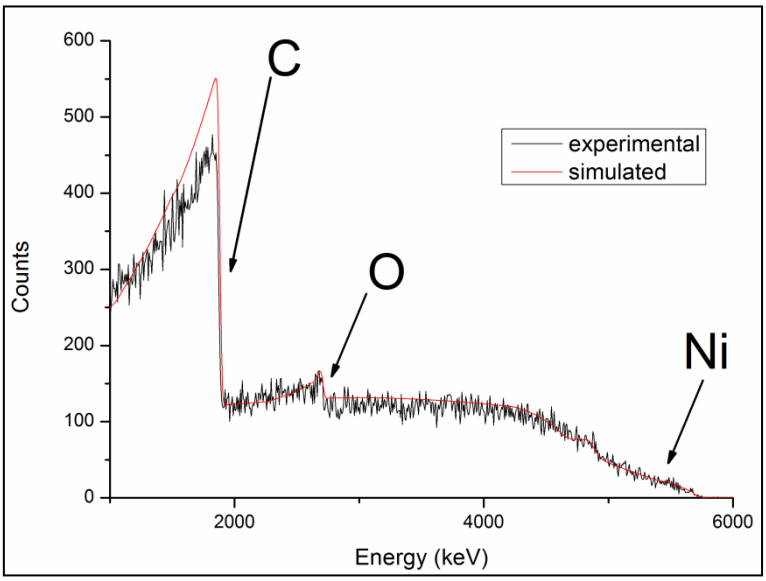

Figure 16: Non Rutherford Elastic Scattering Spectrometry (NRBS) experimental spectrum and simulated spectrum (with SIMNRA) of the uniform deposit formed on the nickel foil (incident He^{2+} beam energy of 7.5 MeV, θ = 172°).

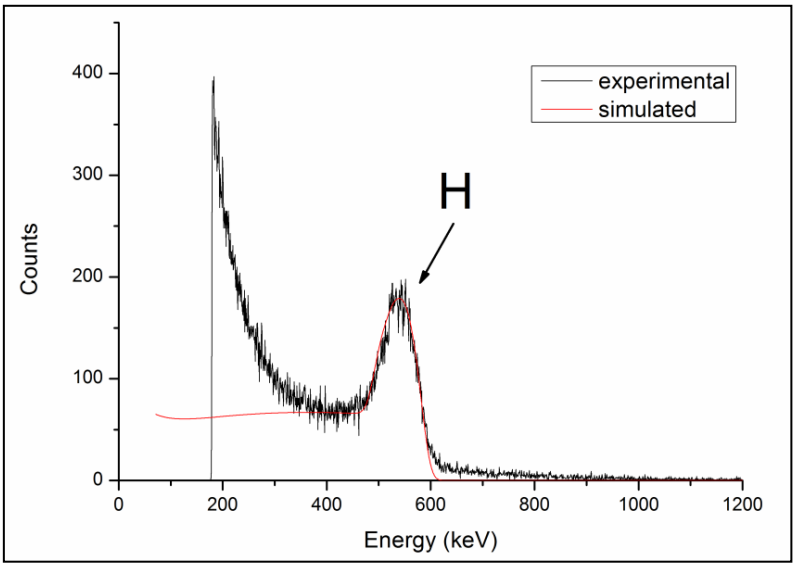

Figure 17: Elastic Recoil Detection Analysis (ERDA) experimental spectrum and simulated spectrum (with SIMNRA) of the uniform deposit formed on the nickel foil (incident He^+ beam energy of 1.7 MeV, θ = 30°, mylar foil thickness = 6.5 µm).

The processing of the simulated spectra leads to following elemental concentrations in the deposit: around 91 at. % carbon, 1.2 at. % oxygen and 6.5 at. % hydrogen.

The concentration profiles of carbon, nickel and hydrogen in function of depth are presented respectively in Figures 18 and 19. It must be noted that the analyzed depth for hydrogen is only about 150 nm whereas it reaches several micrometers for carbon and nickel.

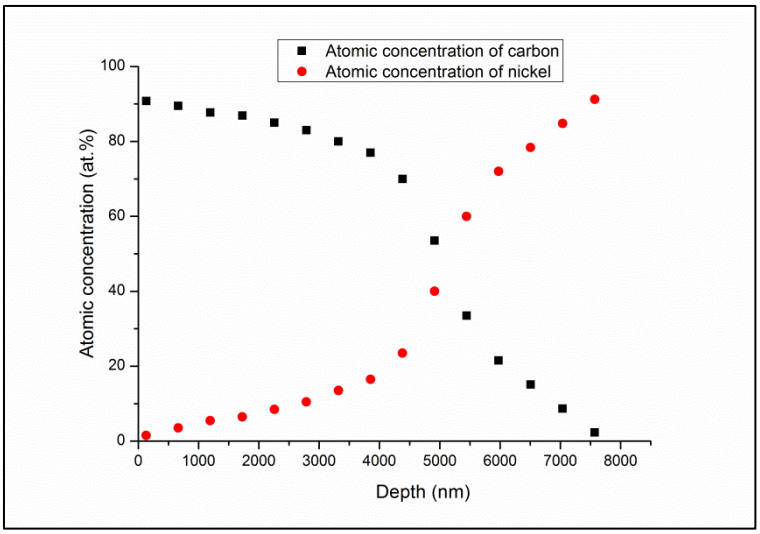

Figure 18: Depth concentration profiles of carbon and nickel in the hydrogenated carbonaceous deposit formed on the heated nickel foil by irradiating a gas mixture CH_4/CO_2 (50/50) with a He^{2+} beam (assuming a density of 1.5 for the deposit).

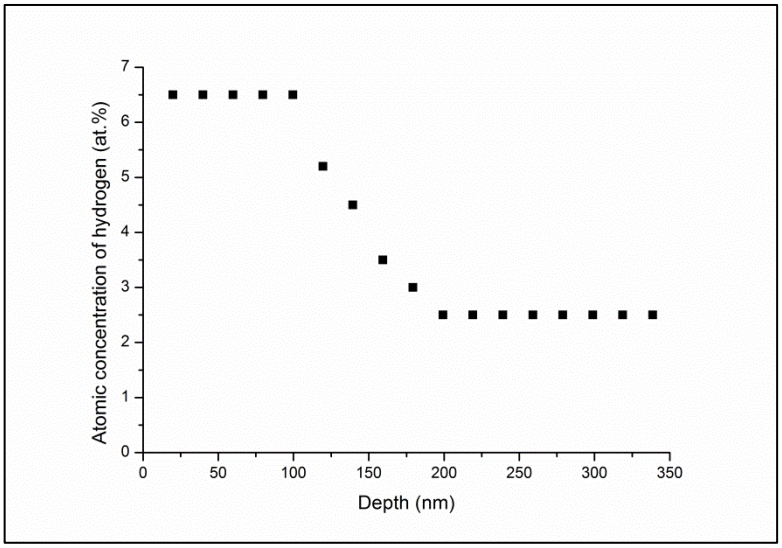

Figure 19: Depth concentration profiles of hydrogen in the hydrogenated carbonaceous deposit formed on the heated nickel foil by irradiating a gas mixture CH_4/CO_2 (50/50) with a He^{2+} beam (assuming a density of 1.5 for the deposit).

3.2.2.3 Secondary Electron Microcroscopy (SEM) and Transmission Electron Microscopy (TEM) characterizations

The uniform deposits have been observed by SEM and TEM. The SEM analyses have been carried out with Dr. A. Perrat Mabilon using a FEI QUANTA 250 FEG at the "Centre Technologique des Microstructures (CTμ)" at University Lyon 1. The HRTEM analyses have been performed by Dr. Jean Noël Rouzaud of the "Laboratoire de Géologie" (ENS Paris) and have been carried out at the "Laboratoire de Réactivité de Surface" at Pierre and Marie Curie University, Paris.

The SEM images show a weblike network of carbonaceous filaments and tubes of some micrometers (Figures 20 and 21).

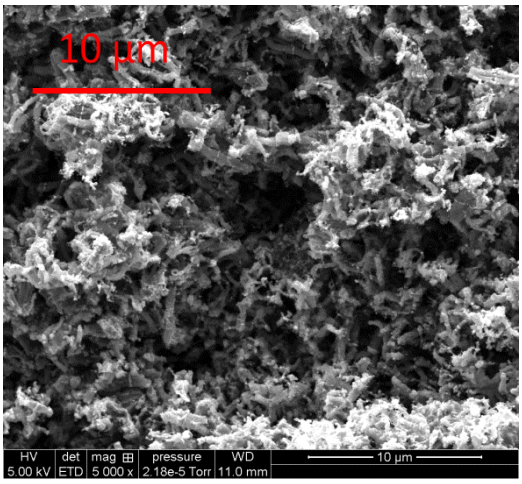

Figure 20: SEM image of the deposit on the nickel foil (HV 5 kV, magnification 5000)

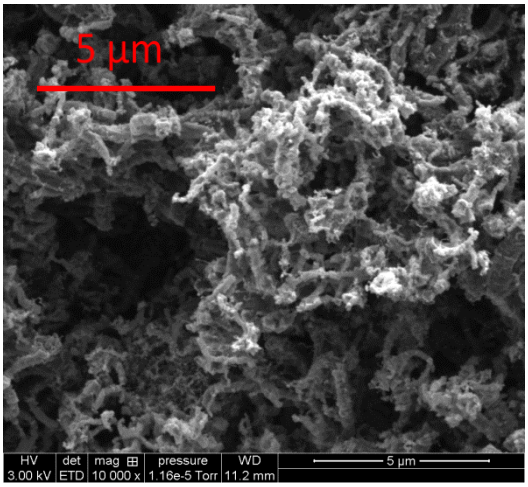

Figure 21: SEM image of the deposit on the nickel foil (HV 3kV, magnification 10000)

The HRTEM images of the deposits formed on the nickel foil reveal the presence of many nanofibers for which most of the graphene planes are perpendicular to the axis of the fiber and of some nanotubes for which most of the graphene planes are parallel to the axis of the tube (Figure 22). The nickel substrate catalyzed the formation of the deposit as it can be seen in Figure 22 (left picture) where the nickel appears in dark color.

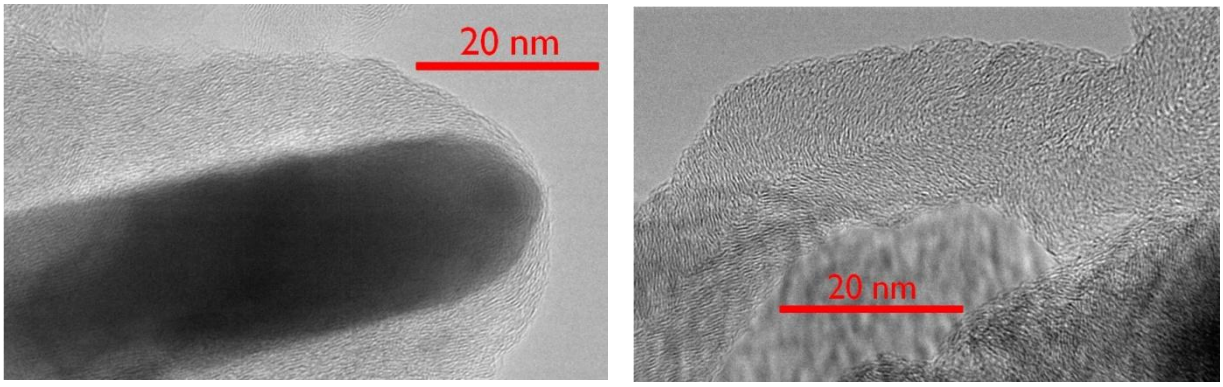

Figure 22 left and right: HRTEM pictures of nanofibers grown on a nickel plate heated at 500°C and irradiated with He^{2+} together with a gas mixture of CH_4/CO_2.

The SEM characterization of the deposits formed on the HOPG surface confirmed the heteregeneous distribution of the deposit occuring on the fractures as spherical "wool balls" where the nanotubes or nanofibers can be distinctively observed (Figures 23). The pictures show that the thickness of the tubes or fibers reaches around 100 nm and their length reaches several hundred of nanometers.

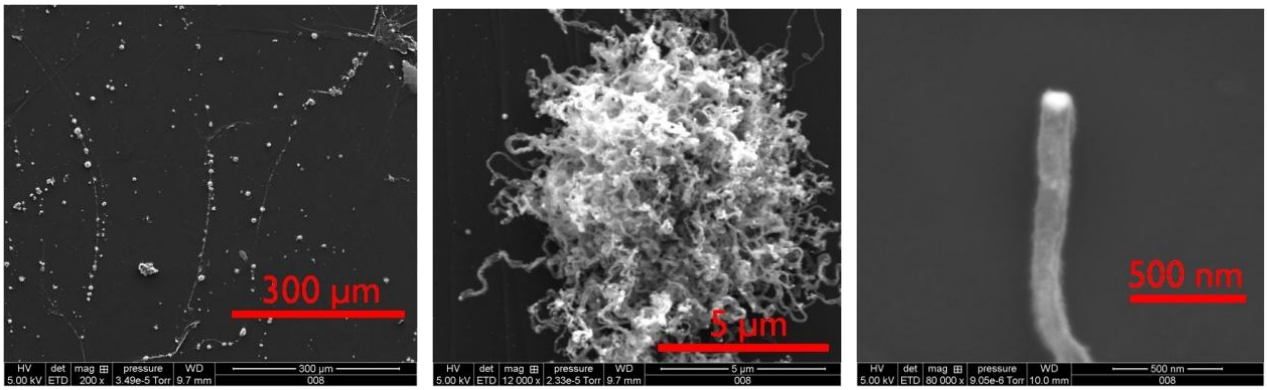

Figure 23 left, middle, right: SEM pictures of the deposit on HOPG, HV 5 kV, respective magnifications of 200, 12000 and 80000.

3.2.2.4 Raman microspectroscopy

The Raman microspectroscopy analyses have been performed by Dr. Jean Noël Rouzaud and D. Deldicque of the "Laboratoire de Géologie" (ENS Paris) with a Renishaw InVia spectrometer using a laser wavelength of 514.5 nm. The analyzed surface and mean depth were respectively around 1µm^2 and 0.2 nm. Figure 24 represents the experimental and fitted first order Raman spectra of the carbonaceous deposit. It displays the "graphite band" G as well as additional "defect bands" D1 to D4 which are characteristic of disordered graphite [A. Sadezky et al. 2005]. The broad defect bands can be interpreted in terms of highly disordered graphite structures as those observed for soots by A. Sadezky et al. [A. Sadezky et al. 2005].

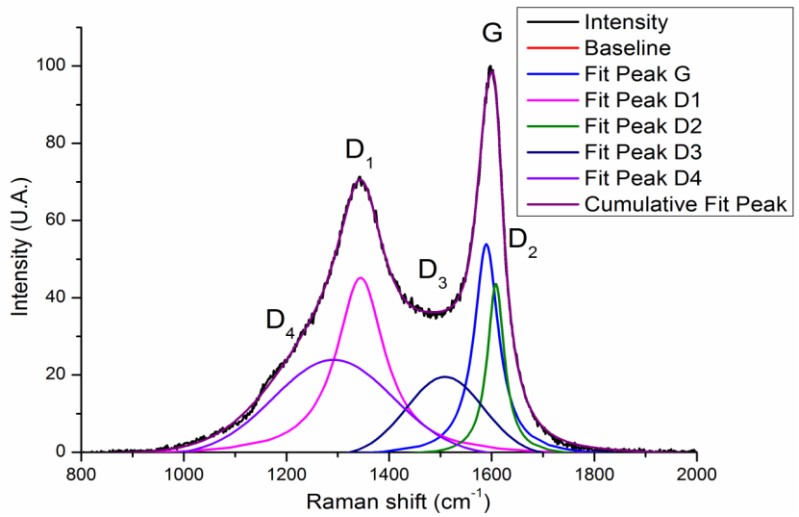

Figure 24: Experimental and fitted first order Raman spectra of the carbonaceous deposit (λ=514 nm)

3.3 Dissolution of the carbon suboxide and the hydrogenated carbonaceous deposits in water:

The dissolution properties of both types of carbon deposits in pure water were tested.

Therefore, the glass slide with the carbon suboxide deposit (Figure 25) was put in contact with demineralized water.

When a drop of water was put in contact with the deposit, the pH dropped to 3 in the water droplet and when the deposit was immersed into water it dissolved very rapidly (Figure 26 respectively left and right pictures).

Figure 25: Carbon suboxide deposit on a glass slide

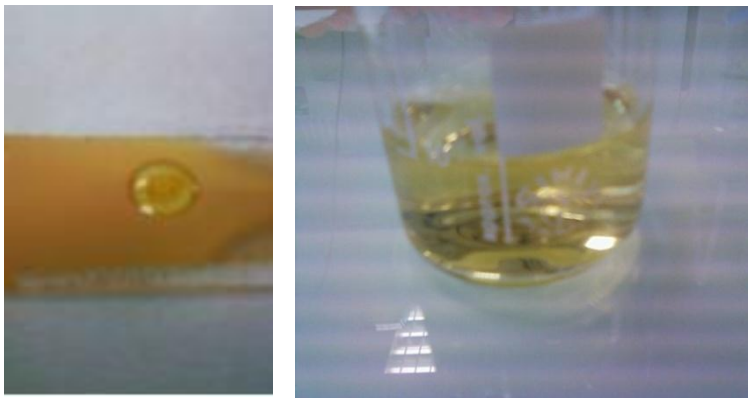

Figure 26: Dissolution of the carbon suboxide deposit in a water droplet (left picture) and demineralized water (right picture)

As for the hydrogenated carbonaceous deposit, the nickel foil covered with the deposit was immersed into demineralized water and the result showed that no dissolution of the deposit occurred, even after several weeks (Figure 27).

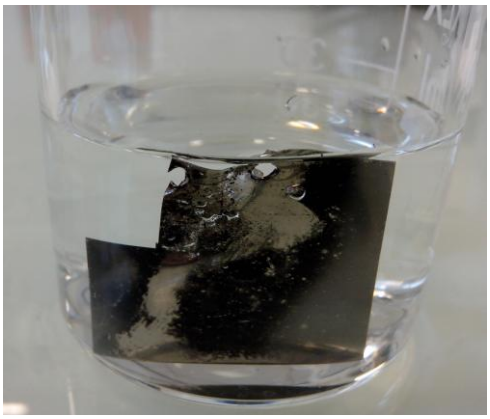

Figure 27: Result of the immersion of the hydrogenated carbonaceous deposit in demineralized water after several weeks

4. Conclusion

Two types of carbon deposits have been synthetized after gas irradiation with He^{2+} ion beam of some MeV: carbon suboxide resulting from the irradiation of carbon monoxide on one hand and hydrogenated carbonaceous deposits resulting from the irradiation of a methane/carbon dioxide (50/50) gas mixture on the other hand.

The carbon suboxide has been derived from the radiolysis of carbon monoxide after its irradiation. C_3O_2 polymerized on substrates such as the metallic walls of the irradiation cell or a glass slide and a nuclear graphite sample introduced into the cell, forming a rusty colored deposit. This suboxide has a hygroscopic nature and literature data point out its progressive decomposition through oxidation at reactor temperatures. These features indicate the labile nature of this kind of deposits in reactor conditions and enlight the fact that its occurence should not be predominant at least on the hotest parts of the reactor. However, their consumption might leave pulverulent carbon particles.

The hydrogenated carbonaceous deposits resulted from the radiolytic destruction of methane. It was initiated by the attack on methane of oxidizing species derived from the radiolysis of carbon dioxide giving higher molecular weight hydrocarbons which subsequently decompose on surfaces. Uniform black colored deposits have been obtained on nickel foils heated at 500°C during irradiation. Indeed, the formation of these deposits are known to be catalyzed by transition metals. The irradiation of highly ordered pyrolitic graphite (HOPG), also heated up to 500°C during irradiation, led to the formation of "urchin-shaped" black deposits located on fractures. HRTEM showed that the deposit formation was catalyzed by nickel and led to the formation of nanofibers with some nanotubes. Concerning for the deposit formed on HOPG, SEM pictures seem to point out spherical "wool-balled" nanotubes or nanofibers. This kind of deposit is therefore likely to form preferentially on hot metallic parts in the reactors but may also occur on graphite to a lesser extent.

The immersion of the two kinds of deposits into demineralized water shows that the carbon suboxide deposits are very soluble in pure water, whereas the hydrogenated carbonaceous deposits are almost insoluble. Knowing that the deposits might have incorporated radioactive nuclides such as ^{14}C or ^{36}Cl, these properties should be considered for dismantling under water and to foresee the disposal options or the long term disposal behaviour of irradiated graphite.

References

[G.C. Allen et al. 1997] : Carbon deposition from a γ irradiated $CO_2/CO/C_2H_4/C_2H_6$ gas mixture on the manganese oxides MnO, Mn_3O_4 and Mn_2O_3, Journal of Nuclear Materials (1997) 250, 111-117

[T.Baird et al. 1980]: T.Baird et al., "Carbon Deposition on Metals", *Proceedings of the Conference on Gas Chemistry in nuclear reactors and large industrial plants, Salford*, 34-39, 1980

[R.T.K.Baker et al. 1972]: R.T.K.Baker et al., "Nucleation and growth of carbon deposits from the nickel catalyzed decomposition of acetylene", *Journal of Catalysis*, Vol 26, 51-62, 1972

[C.J. Bennett et al. 2008]: Mechanistic studies on the decomposition of carbon suboxide in a cometary ice analog, Planetary and Space Science 56 (2008) 1181–1189

[A. R. Blake, et al. 1963]: Carbon Suboxide Polymers. Part 1.-Structure of Thermal Polymers, Trans. Faraday Soc. 60: 691

[A.Blanchard et P.Campion 1980]: A.Blanchard et P.Campion, "Carbon deposition on 20/25/Nb steel using an electrically heated AGR fuel pin", *Proceedings of the Conference on Gas Chemistry in nuclear reactors and large industrial plants, Salford,* 90-97, 1980

[R.Blanchard et al. 1969] : R.Blanchard et al., " Etude des dépôts par oxydation thermique différentielle et par dégazage", *CEA Département de Physico-Chimie Service de Physico-Chimie Appliquée* , DPC/PCA/70-15/PL/ES, Rapport numéro 734, 15/01/1970

[R.Blanchard et al. 1971] : R.Blanchard et al., "Corrosion du graphite et dépôts hydrogénés dans le réacteur Bugey", CEA *Département de physique des réacteurs et de mathématiques appliquées Service d'Etudes de Réacteurs et de Mathématiques Appliquées et Département de métallurgie de Grenoble Service d'Elaboration et de Radio-Métallurgie*, CEA/DEDR/Rapport SERMA/D.R/N°15/71 et CEA/DMECN/Rapport DMG/D.R/N°37/71, 01/01/1971

[J.Brisbois et C.Fiche 1967] : J.Brisbois et C.Fiche, "Bilans énergétiques, corrosion du graphite dans Bugey 1", *Note CEA-N 828 Centre d'Etudes Nucléaires de Fontenay-aux–Roses Département des Etudes de Piles Service d'Etudes de Protection de Piles*, 1-16, 11/1967

[P.Campion 1980]: P.Campion, "Carbon formation processes revelant to advanced carbon dioxide-cooled reactors", *Proceedings of the Conference on Gas Chemistry in nuclear reactors and large industrial plants, Salford,* 53-66, 1980

[A.Dyer et G.E.Moores 1977] : A.Dyer et G.E.Moorse, "The radiolysis of simple gas mixtures_I. Rates of production and destruction of methane in mixtures with carbon dioxide as a mojor constituant", *Radiation Physics and Chemistry*, Vol 20, Issue 5-6, 315-321, 1977

[EPRI Technical Report 2006]: Graphite Decommissioning Options for Graphite Treatment, Recycling or Disposal, including a discussion of Safety-Related Issues, **1013091,** Final Report, March 2006

[R.L.Faircloth et al. 1980]: R.L.Faircloth et al., "Coolant chemistry of the advanced carbon dioxide cooled reactor", *Specialists meeting on coolant chemistry, plate-out and decontamination in gas-cooled reactors Juelich, Federal Republic of Germany IAEA*, B 9-06,125-131, 02/12/1980

[A. Faucitano et al.1977]: Study on the possibilities of isotopic exchange between C_30_2 and CO labelled with ^{14}C in the presence and absence of ionizing radiation, NASA Technical translation, NASA TT F-17435

[C.W.Keep et al. 1980]: C.W.Keep et al., "The effect of surface pretreatment on the growth of carbon onto stainless steel from the decomposition of propane", *Proceedings of the Conference on Gas Chemistry in nuclear reactors and large industrial plants, Salford*, 40-44, 1980

[Lejeune et al. 1974] : Lejeune et al., "Dépôts sur gaine Chinon 2", *Compte rendu de réunion tenue à Chinon*, C 135-01, 1-5, 26/11/1974

[Lejeune et al. 1975] : Lejeune et al., "Dépôts sur gaine Chinon 2", *Compte rendu de réunion tenue à Chinon*, CEA/DEDR/CRG/75-073/BB/YR, 1-8, 28/02/1975

[M. Mayer, SIMNRA]: version 5.0 User's Guide, © Max-Planck-Institut für Plasmaphysik, 1997-2002: www2.if.usp.br/~lamfi/guia-simnra.pdf.

[C.R. Morcombe et al. 2003] : Chemical shift referencing in MAS solid state NMR. J. Magn. Reson. 162:479-486.

[D.J.Norfolk et al. 1980a]: D.J.Norfolk et al., "Mechanisms involved in radiolytic carbon deposition from $CO_2/CO/CH_4$" *Proceedings of the Conference on Gas Chemistry in nuclear reactors and large industrial plants, Salford*, 67-74, 1980

[D.J.Norfolk et al. 1980b]: D.J.Norfolk et al., "Carbonaceous deposition during irradiation of CO2 containing small quantities of CH4 and CO", *Carbon Conference de Baden-Baden*, 263-266, 01/01/1980

[D.J.Norfolk et al. 1983]: D.J.Norfolk et al., "Hydrocarbon chemistry in irradiated $CO_2/CO/CH_4/H_2O/H_2$ Mixtures_1. A survey of the initial reactions", *Radiation Physics and Chemistry*, Vol 21, Issue 3, 307-319, 1983

[C. Pichon, 2006] : Inhibition de la production d'hydrogène radiolytique dans les déchets nucléaires de type «enrobés bitumineux» : étude de l'interaction entre l'hydrogène et l'hydroxosulfure de cobalt, PhD thesis, Ecole Nationale Supérieure des Mines de Saint Etienne

[A. Sadezky et al. 2005]: Raman microspectroscopy of soot and related carbonaceous materials: Spectral analysis and structural information, Carbon 43, 1731-1742

[M.Schmidt 1964]: M.Schmidt, "Polymérisation thermique et sous rayonnement du sous-oxyde de carbone", *Thèse en chimie tinctoriale*, Mars 1964

[R. N. Smith et al. 1963]: The structure and properties of carbon suboxide polymer, Inorganic Chemistry, 2 829.

[A.J.Wickham et al. 1977]: A.J.Wickham et al., "Recent advances in the theories of carbon dioxide radiolysis and radiolytic graphite corrosion", *Radiation Physics and Chemistry*, Vol 10, 107-117, 1977

[C.J.Wood 1980]: C.J.Wood, "Coolant chemistry in CEGB reactors", *Proceedings of the Conference on Gas Chemistry in nuclear reactors and large industrial plants, Salford*, 6, 1980

[J.Wright 1980]: J.Wright, "Historical introduction to gas chemistry in nuclear reactors", *Proceedings of the Conference on Gas Chemistry in nuclear reactors and large industrial plants, Salford*, 1-5, 1980

[M.Yvars et al. 1973] : M.Yvars et al., "Caractéristiques physico-chimique des dépôts carbonés obtenus par radiolyse de l'oxyde de carbone. Oxydation des dépôts", *CEA Département de technologie Service de Physico-Chimie des Matériaux*, D.TECH/SPCM/73-225/MY/ES, Note technique numéro 904, 10/04/1973